Unraveling the Molecular Mechanism of pH-Induced Misfolding and Oligomerization of the Prion Protein

Jogender Singh and Jayant B. Udgaonkar

National Centre for Biological Sciences, Tata Institute of Fundamental Research, Bengaluru 560065, India

Correspondence to Jayant B. Udgaonkar: *jayant@ncbs.res.in*
http://dx.doi.org/10.1016/j.jmb.2016.01.030
Edited by S. Radford

Abstract

The misfolding of the prion protein (PrP) to aggregated forms is linked to several neurodegenerative diseases. Misfolded oligomeric forms of PrP are associated with neurotoxicity and/or infectivity, but the molecular mechanism by which they form is still poorly understood. A reduction in pH is known to be a key factor that triggers misfolded oligomer formation by PrP, but the residues whose protonation is linked with misfolding remain unidentified. The structural consequences of the protonation of these residues also remain to be determined. In the current study, amino acid residues whose protonation is critical for PrP misfolding and oligomerization have been identified using site-directed mutagenesis and misfolding/oligomerization assays. It is shown that the protonation of either H186 or D201, which mimics the effects of pathogenic mutations (H186R and D201N) at both residue sites, is critically linked to the stability, misfolding and oligomerization of PrP. Hydrogen–deuterium exchange studies coupled with mass spectrometry show that the protonation of either H186 or D201 leads to the same common structural change: increased structural dynamics in helix 1 and that in the loop between helix 1 and β-strand 2. It is shown that the protonation of either of these residues is sufficient for accelerating misfolded oligomer formation, most likely because the protonation of either residue causes the same structural perturbation. Hence, the increased structural dynamics in helix 1 and that in the loop between helix 1 and β-strand 2 appear to play an early critical role in acid-induced misfolding of PrP.

Introduction

The misfolding of the mainly α-helical, monomeric cellular prion protein, PrP^C, into the mainly β-structured, multimeric PrP^{Sc} form is linked with several fatal neurodegenerative diseases in humans and other mammals [1]. Despite PrP^{Sc} being clearly involved in prion pathogenesis, its size and structure are not yet well known [2]. Although the accumulation of insoluble, protease-resistant PrP^{Sc} in the central nervous system is thought to be a characteristic feature of prion diseases, soluble oligomeric forms that may [3] or may not [4] be protease resistant have been shown to be neurotoxic and infectious [5–9].

Recombinant PrP forms misfolded oligomers *in vitro* in the presence of 150 mM NaCl [10,11]. Misfolded oligomer formation is facilitated by a lowering of pH. Importantly, oligomers formed *in vitro* at low pH have been shown to be cytotoxic [5,12], and prion disease susceptibility appears to correlate well with the propensity of recombinant PrP to form these oligomers [13]. The oligomers formed at low pH can disrupt lipid membranes [11,14,15], pointing toward a putative mechanism of their toxicity. Although it is evident now that the misfolded oligomeric forms play key roles in neurotoxicity and/or infectivity *in vivo*, as well as in cytotoxicity *ex vivo*, the molecular details of the conversion of monomeric PrP into misfolded oligomers are not well understood [16].

In vitro, the aggregation of PrP is highly dependent on the environmental conditions [10,16,17]. At neutral or slightly acidic pH, PrP forms amyloid fibrils. *In vivo* as well, GPI-anchorless PrP transgenic mice have been shown to have large quantities of fibrillar PrP^{Sc} extracellularly where the pH is neutral [18]. At low pH, PrP forms misfolded β-rich
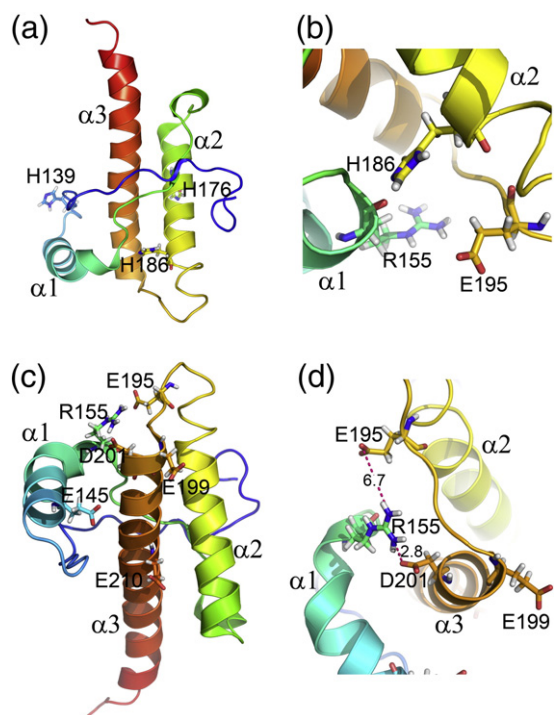
Fig. 1. Structure of the CTD (residues 121–231) of the mouse prion protein. Mutation sites have been labeled. The residue stretch 23–120 is known to be unstructured in the full-length protein. The color gradient is from blue (N-terminus) to red (C-terminus). (a) Different His residues, which were mutated in the current study, are labeled. The side chains of H139, H176 and H186 are buried to the extents of 16%, 19% and 78%, respectively. (b) A close-up of the region near residue H186. (c) Different acidic and basic residues, which were mutated in the current study, are labeled. The side chains of E145, R155, E195, E199, D201 and E210 are buried to the extents of 99%, 63%, 47%, 0%, 100% and 63%, respectively. (d) A close-up of the region near residue R155. The distances between the side chains of R155-E195 and R155-D201 are shown in angstroms (Å). The figure was drawn using the program PyMOL and the PDB file 1XYX.

oligomers. The formation of misfolded oligomers has been shown to be linked with the protonation of at least one critical residue. The amount of misfolded oligomer increases with decreasing pH, with the pH-induced transition characterized by an apparent pK_a of 4.7 [11]. Interestingly, aggregation of PrP has been shown to occur in the endocytic pathway [19,20] in which lysosomes have a low internal pH. It is likely that PrP misfolds to oligomeric forms when it encounters acidic pH in the endocytic pathway. Identification of the residues whose protonation is linked to misfolding and oligomerization and determination of the structural effects of this protonation are critical steps in achieving an understanding of the mechanism of conformational conversion of PrP.

The apparent pK_a of 4.7 for misfolded oligomer formation [11] suggests that the protonation of one or

more His residues with reduced pK_a values and/or the protonation of one or more buried Asp or Glu residues with elevated pK_a values is important in conformational conversion. In either case, the pK_a values of the critical residue side chain could be different in the monomer and in the oligomer. Molecular dynamics (MD) simulations have suggested that H154 and H186 (mouse numbering; mouse numbering has been used throughout this article) could be the critical residues in the case of human PrP [21]: the apparent pK_a values for their protonation were determined by MD simulations and NMR measurements to be ~ 4.5–5.0 [21,22]. The H186R mutation, which mimics protonated H186, is linked with familial Creutzfeldt–Jakob disease [23] and shows increased misfolding [24], indicating that the protonation of H186 might be important for the misfolding of PrP. However, H139 also shows a pK_a value, as measured by NMR [22], similar to that of H186, indicating that its protonation might also be important. Hence, the importance of the protonation of different His residues in PrP misfolding is not clear. The structural consequences of the protonation of His residues are also not yet well understood.

Several familial prion diseases are caused by pathogenic mutationsinvolving replacement of acidic amino acid residues by either neutral or basic amino acid residues [25]. Removal of a negative charge by these pathogenic mutations mimics a reduction in pH that would neutralize the charge. The removal of a negative charge is likely to disrupt electrostatic interactions, but a clear picture about the roles of different acidic amino acid residues in the misfolding of PrP is yet to emerge.

In the current study, amino acid residues whose protonation is critical for misfolding and oligomerization have been identified in the mouse prion protein (moPrP). By employing point mutations, it is shown that only the protonation of H186 leads to a drastic destabilization and increased misfolding rate of the protein although three His residues are present in the structured C-terminal domain (CTD) of moPrP. In addition, it is shown that the R155-D201 salt bridge is critical for the stability and misfolding of moPrP. Replacement of either R155 or D201 by a neutral residue destabilizes the protein and increases its misfolding rate drastically. Hydrogen–deuterium exchange (HDX) studies coupled with mass spectrometry (MS) show that helix 1 (α1) and the loop between α1 and β-strand 2 (β2) are destabilized upon protonation of either H186 or D201, along with regions in the proximity of the mutations. The results of the structural dynamics studies suggest a model for the pH-induced misfolding and oligomerization of moPrP.

Results and Discussion

To understand how the protonation of the His residues present in the CTD of moPrP affects its
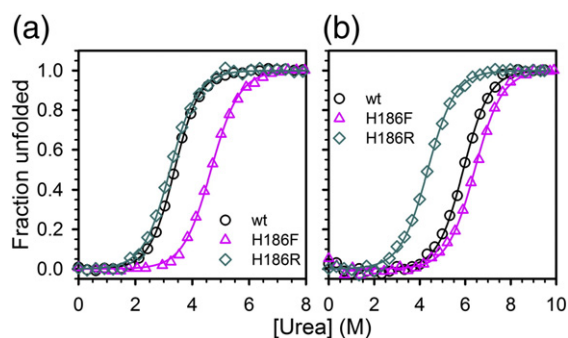
Fig. 2. Effect of the protonation of residue 186 on the stability of moPrP. Urea-induced equilibrium unfolding transitions of different moPrP variants at pH 4 (a) and pH 7 (b), 25 °C as monitored by far-UV CD at 222 nm. The side chain of residue 186 becomes positively charged in wt moPrP at pH 4 and in H186R moPrP at both pH 4 and pH 7.

misfolding and oligomerization, they were replaced with neutral amino acid residues, one at a time. There are three His residues in the CTD of moPrP at positions 139, 176 and 186 (Fig. 1a and b). Unlike human PrP, moPrP does not have a His residue at position 154. Three mutant proteins, H139Q, H176F and H186F, were generated. Phe has a size and helix-forming propensity comparable to those of His, and hence, His was replaced with Phe at positions 176 and 186. Since a Phe residue is present at position 140, H139 was replaced with Gln, which has a comparable size to His, in order not to have two adjacent aromatic amino acid residues. All three mutant proteins show far-UV circular dichroism (CD) spectra similar to that of wild-type (wt) moPrP under native conditions (Fig. S1a), indicating that these mutations do not alter the overall secondary structure of moPrP.

The CTD of moPrP has several other ionizable residues (Table S1) including acidic residues, whose protonation could facilitate misfolding and oligomerization. Some of these ionizable residues are present in salt bridges; MD simulations have suggested that salt bridges are important for the stability of PrP [26,27]. To probe the roles of different acidic residues, moPrP variants, either with mutations of residues involved in the formation of salt bridges important for tertiary structure (E145Q moPrP) or with mutations linked to familial prion diseases (E195K, E199K, D201N and E210Q moPrP) were made (Fig. 1c and Table S1).

H186F moPrP shows a drastic increase in thermodynamic stability at pH 4 but not at pH 7

Urea-induced equilibrium unfolding studies showed that both H139Q and H176F moPrP are about as stable as wt moPrP at pH 4 (Fig. S1b and Table S2). On the other hand, H186F moPrP was

substantially more stable than wt moPrP at pH 4 ($\Delta\Delta G$ = +1.75 kcal/mol) (Fig. S1b and Table S2). H186F moPrP also showed a drastic increase in its melting temperature (T_m), while H139Q and H176F moPrP showed T_m values similar to that of wt moPrP (Fig. S1c and Table S2). In contrast to the results at pH 4, H186F moPrP was only slightly more stable than wt moPrP at pH 7 (Fig. 2 and Table S3). This indicated that H186 does not become protonated in wt moPrP at pH 7; consequently, wt moPrP is about as stable as H186F moPrP at pH 7. These results suggested that, in wt moPrP, the protonation of H186, which occurs at pH 4 but not at pH 7, causes a drastic reduction in the stability of the protein. Interestingly, a recent study shows that the replacement of H186 by Tyr also stabilizes moPrP at low pH [28], suggesting that the stabilization effect is independent of the residue introduced.

H186R moPrP shows a drastic reduction in the stability at pH 7 but not at pH 4

If protonation of H186 leads to destabilization of moPrP, then the protein should get destabilized even at pH 7 if residue 186 could be given a positive charge at that pH. H186R is a pathogenic mutation that introduces a positive charge at residue 186 at pH 7. Urea-induced equilibrium unfolding studies showed that H186R moPrP was as stable as wt moPrP at pH 4 (Fig. 2a) but was much less stable than wt moPrP at pH 7 (Fig. 2b and Table S3). Hence, the introduction of a positive charge on the side chain of residue 186 in moPrP, either on a protonated H186 (at pH 4) or on a protonated R186 (at pH 4 or 7), leads to a drastic destabilization of the protein.

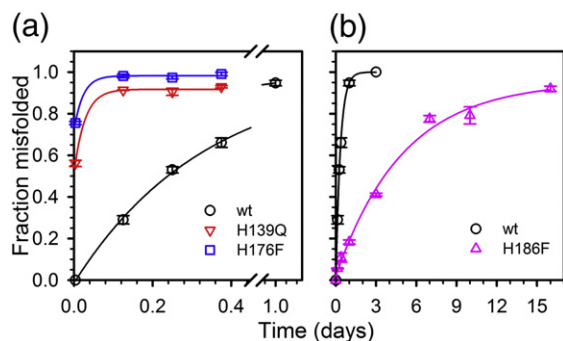### H186F moPrP shows reduced misfolding rates while H139Q and H176F moPrP show increased misfolding rates

The effects of mutations of His to neutral residues on the misfolding and oligomerization of moPrP in the presence of 150 mM NaCl, at 37 °C (pH 4) and at 100 μM protein concentration, were studied using far-UV CD (Fig. S2) and size-exclusion chromatography (SEC) (Fig. S3a). Far-UV CD spectra showed that the oligomer formed at different times was β-rich, while the monomer was α-helical (Fig. S2). The morphology and size of moPrP oligomers formed under the abovementioned conditions have been characterized in detail in an earlier study [29]. moPrP forms spherical oligomers, which have a hydrodynamic radius of 10–12 nm [29]. Other studies have also shown that, under similar conditions of oligomer formation, PrP forms oligomers of similar sizes (10–12 nm hydrodynamic radius) [30,31]. H139Q and H176F moPrP misfolded and oligomerized very much faster than wt moPrP
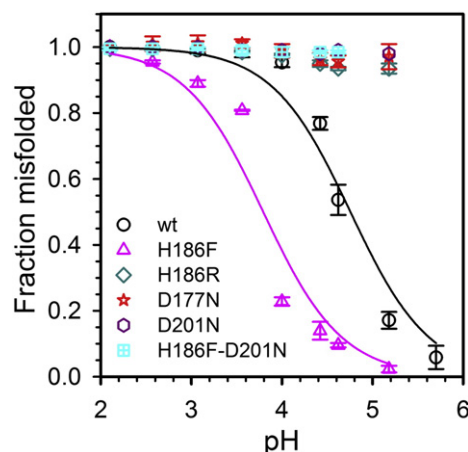
(Fig. 3a and Fig. S3b), suggesting that the proton-ation of H139 or H176 in wt moPrP would not increase the misfolding and oligomerization rates. It is possible that the protonation of H139 or H176 might instead decrease the rates of misfolding and oligomerization of wt moPrP. However, if this were the case, the protonation would most likely be through affecting intermolecular association steps after the initial conformational change, as both H139Q and H176F moPrP are as stable as wt moPrP (Table S2). In this context, it should be noted that several MD studies [32,33] have suggested that the protonated forms of these residues form salt bridges with different residues. In contrast to H139Q and H176F moPrP, H186F moPrP showed a drastic reduction in the misfolding and oligomerization rates (Fig. 3b and Fig. S3c).

H186R moPrP misfolds in a pH-independent manner

moPrP forms misfolded oligomers in a pH-dependent manner [11]. In the presence of 150 mM NaCl at 37 °C and at 100 μM concentration, wt moPrP showed an apparent pK_a for the misfolding transition of ~4.7 (Fig. 4). If this transition is caused by the protonation of H186, then H186R moPrP should misfold completely in a pH-independent manner in the acidic pH range, as this mutant variant would mimic wt moPrP with a protonated H186. To probe if that is true, a pH titration of the misfolding of H186R moPrP was carried out under the same conditions as for wt moPrP. H186R moPrP was found to be

Fig. 4. pH dependence of the misfolding of moPrP variants. Fraction misfolded form at 24 h is plotted *versus* pH. The fraction misfolded form was calculated by using the fractional change in the CD signal at 222 nm. The lines through the data points for wt and H186F moPrP represent fits to Eq. (1) (Materials and Methods). Error bars represent the spread in data from two independent experiments. It was not possible to obtain data for several of the mutant variants above pH 5.2 because of solubility problems.

completely misfolded in the pH range 2–5.2 (Fig. 4), above which it precipitated out of solution. This result showed that the protonation of H186, or the introduction of a positive charge on the side chain of residue 186, is critical for moPrP misfolding.

H186F moPrP has reduced structural dynamics in α1, the loop between α1 and β2, the C-terminus of α2 and the loop between α2 and helix 3 (α3) at pH 4

To understand why H186F moPrP misfolds slower than wt moPrP at pH 4, it was important to determine the structural differences between H186F and wt moPrP. To this end, HDX-MS studies were carried out to obtain sequence-specific information about the structural changes. In HDX studies, structured regions of the protein are generally protected against HDX; unstructured, solvent-exposed regions become labeled with deuterium. The labeled segments show an increase in mass and can be identified by carrying out peptic digestion at low pH, where the exchange reaction is quenched. In this way, localized information about the structural dynamics of different parts of the protein can be obtained. A peptide map generated earlier [15] was used for the current study. For HDX-MS studies, the native monomeric protein in H_2O buffer was diluted 20 times in D_2O buffer at pH 4. Since pH 4 is not far from the pH at which intrinsic HDX rates are at their minimum, HDX can be observed at a large number of amide hydrogen sites, spread over all the secondary structural elements of the protein.

Fig. 3. Effect of His mutations on the misfolding of moPrP. (a) Fraction misfolded form at different times of aggregation of wt, H139Q and H176F moPrP at 100 μM concentration in 150 mM NaCl at 37 °C, pH 4. (b) Fraction misfolded form at different times of aggregation of wt and H186F moPrP at 100 μM concentration in 150 mM NaCl at 37 °C, pH 4. The fraction misfolded form was calculated by using the fractional change in the CD signal at 222 nm. The continuous lines through the data points in both the panels were drawn by inspection to guide the eye. Error bars represent the spread in data from two independent experiments.

The kinetics of deuterium incorporation in the sequence segments covering α1, the loop between α1 and β2, the C-terminus of α2 and the loop between α2 and α3 were found to be slower for H186F moPrP than for wt moPrP at pH 4 (Fig. 5). This suggested that the protonation of H186 in wt moPrP leads to increased structural dynamics in these regions. MD simulations suggest that the protonation of H186 disrupts the electrostatic network and other interactions between the C-terminus of α2 and the loop between α1 and β2 involving residues R155, N158, Q159, E195 and D201 [21,32,34,35]. It is likely that the increased structural dynamics in these regions in wt moPrP mentioned above is due either to the destabilization/unraveling of α1 or to the movement of α1 and the loop between α1 and β2 away from α2. Such a movement would lead to the exposure of the C-terminus of α2, which is highly prone to misfolding, and eventually would lead to the misfolding of moPrP [11,36].

**H186R moPrP has increased structural dynamics in α1, the loop between α1 and β2 and the loop between α2 and α3 at pH 7**

Since the stability of H186R moPrP was found to be substantially lower than that of wt moPrP at pH 7, it was important to characterize the structural

changes that lead to this destabilization. HDX-MS studies were carried out on H186R moPrP at pH 7 using wt moPrP as a reference. The kinetics of deuterium incorporation in the sequence segments covering α1, the loop between α1 and β2 and the loop between α2 and α3 were found to be faster for H186R moPrP than for wt moPrP (Fig. S4). Importantly, these same regions showed increased stability in H186F moPrP at pH 4 (Fig. 5). This result confirmed that the protonation of H186 in wt moPrP leads to increased structural dynamics in these regions.

H186F moPrP oligomerizes rapidly in the presence of denaturants

The HDX-MS studies showed that the structural dynamics in α1, the loop between α1 and β2, the C-terminus of α2 and the loop between α2 and α3 are reduced in H186F moPrP, while they are increased in H186R moPrP. The misfolding/oligomerization rate is also reduced in the former. If it is the increased structural dynamics in α1 and parts of α2-α3, upon protonation of H186, which is responsible for accelerating the misfolding/oligomerization of wt moPrP, then H186F moPrP should also oligomerize rapidly under denaturing conditions where these regions (and other regions) would have increased structural dynamics.
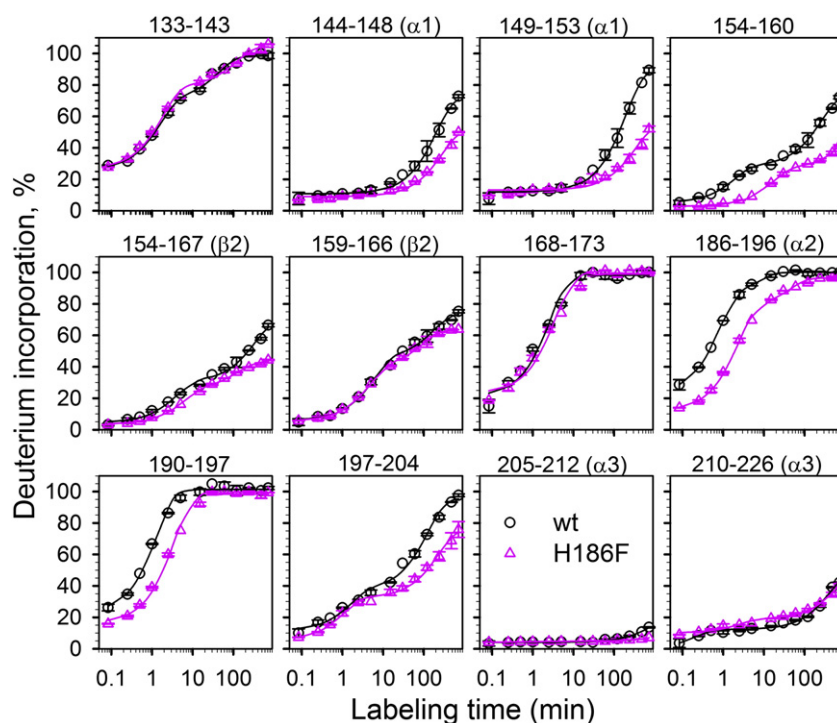
Fig. 5. Time course of HDX into different secondary structural regions of monomeric H186F and wt moPrP at pH 4. Percent deuterium incorporation profiles at pH 4, 25 °C of selected sequence segments, are shown. Error bars represent the spread in data from two independent experiments. The lines through the data represent fits to either a monoexponential or a biexponential equation.

SEC studies showed that, under denaturing conditions [3 M urea, 1 M guanidine hydrochloride (GdnHCl) and 150 mM NaCl, pH 4, at 37 °C] at 100 µM protein concentration, H139Q and H176F moPrP oligomerized very rapidly (data not shown), while H186F moPrP also oligomerized faster, but at a rate similar to that of wt moPrP (Fig. S5). The observation that H186F moPrP oligomerized as rapidly as wt moPrP in the presence of denaturants also suggested that the reduction in oligomerization rate of H186F moPrP in the absence of denaturants is not because of introduction of Phe but because of the removal of His at residue position 186.

Acidic residues in the pH-induced misfolding of moPrP

The characterization of the His mutant variants showed that the protonation of H186 facilitates the misfolding of moPrP. However, it was also important to determine whether the protonation of any other residues also plays a role in misfolding and oligomerization. In particular, since several of the pathogenic mutations of PrP involve mutations of acidic amino acid residues to either neutral or basic residues [25], it was important to determine whether there are acidic residues whose protonation is critical for the misfolding and oligomerization of PrP. The observation that the low pH-induced misfolding transition of H186F moPrP has an apparent pK_a of ~3.8 (Fig. 4) clearly indicates that there are some acidic residues whose protonation is critical for misfolding of moPrP. Indeed, D177N PrP, a pathogenic mutation, is already known to have increased misfolding and oligomerization rates [36,37]. It was found in the current study that D177N moPrP is misfolded completely in the pH range 2–5.2 (Fig. 4). This indicated that protonation of D177 is critical for the misfolding of moPrP.

The R155-D201 salt bridge stabilizes moPrP and prevents its misfolding and oligomerization

The stabilities of several moPrP mutant variants, in which acidic residues were mutated, were checked by urea-induced and thermally induced equilibrium unfolding studies (Fig. S6). All the mutant variants, except for D201N, showed stabilities either similar to or slightly lower than that of wt moPrP (Table S4). D201N moPrP showed a substantial decrease in both the thermodynamic stability and T_m compared to wt moPrP (Table S4). In a recent study, the D201N mutation was shown to destabilize moPrP [36]. MD simulations suggest that D201 makes a strong salt bridge with R155 [27], which is further supported by the close proximity of the two residues in the NMR structure of the protein (Fig. 1d). It is likely that the disruption of this salt bridge is responsible for the substantial decrease in the stability of D201N moPrP.

Thermodynamic stabilities of PrP variants may not correlate with their amyloidogenic propensities [38]. Hence, to know how these mutations affect the misfolding and oligomerization of moPrP, the misfolding and oligomerization of these mutant variants were studied in the presence of 150 mM NaCl, at 37 °C, pH 4 and at 100 µM protein concentration, using CD (Fig. 6) and SEC (Fig. S7a), respectively. For all the mutant variants except D201N, the rates of misfolding and oligomerization were found to be either similar to or only slightly faster than that of wt moPrP (Fig. 6a and Fig. S7b). D201N moPrP showed a drastic increase in the misfolding and oligomerization rates (Fig. 6b and Fig. S7b). Moreover, D201N moPrP was found to be completely misfolded in the pH range from 2 to 5.2 (Fig. 4), indicating that the protonation of D201 is critical for the misfolding of PrP. It seemed that the R155-D201 salt bridge is very crucial for the stability and misfolding of moPrP, and it was therefore predicted that mutation of R155 to a neutral amino acid residue would show an effect similar to that of the D201N mutation. To this end, Arg at residue position 155 was replaced with Gln. R155Q moPrP, which is not known to be linked to any familial prion diseases so far, showed a substantial decrease in its thermodynamic stability and T_m, similar to that shown by D201N moPrP (Fig. S6 and Table S4). Importantly, R155Q moPrP showed a drastic increase in the rate of oligomerization compared to that of wt moPrP (Fig. S7b). The rate of misfolding for R155Q moPrP was even faster than that of D201N moPrP (Fig. 6b), which may be because R155 could also be forming a salt bridge with E195 (Fig. 1d) [26,27]. It should be noted that, in the absence of 150 mM NaCl, both R155Q and D201N moPrP are helical and show far-UV CD spectra similar to that of wt moPrP (Fig S8).

R155Q and D201N moPrP show increased structural dynamics in α1, the loop between α1 and β2 and the loop between α2 and α3

Since the R155-D201 salt bridge is very critical for the stability and misfolding of moPrP, it was important to determine the structural changes that occur upon disruption of this salt bridge. HDX-MS studies were therefore carried out on R155Q and D201N moPrP at pH 4. The sequence segments covering α1, the loop between α1 and β2 and the loop between α2 and α3 in both R155Q and D201N moPrP were found to show increased rates of deuterium incorporation (Fig. 7). In an earlier study as well, D201N moPrP had been shown to undergo similar structural changes [36]. Importantly, these structural changes were found to be similar to the structural changes seen in the protein upon protonation of H186.
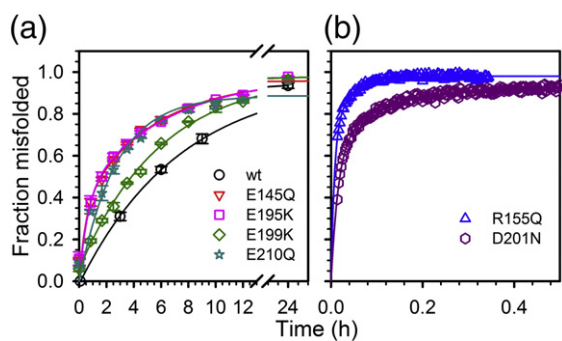
Fig. 6. Effects of mutations of acidic and basic amino acid residues on the misfolding of moPrP. (a) Fraction misfolded form at different times of aggregation as probed by CD at 228 nm of 100 μM protein in 150 mM NaCl at 37 °C, pH 4. (b) Fraction misfolded for R155Q and D201N moPrP. The continuous lines through the data points represent fits to exponential equations. Error bars represent the spread in data from two independent experiments.

Protonation of either H186 or D201 is sufficient for the misfolding of moPrP

wt moPrP showed substantial misfolding at pH 4.4 while H186F moPrP showed negligible misfolding at the same pH (Fig. 4). This indicated that the misfolding of wt moPrP at pH 4.4 was primarily because of protonation of H186. Hence, protonation

of H186 alone, among the critical residues for misfolding, was sufficient for enabling the misfolding of moPrP. To probe whether protonation of just D201 alone was also sufficient for the misfolding of moPrP, the variant H186F-D201N moPrP was generated. H186F-D201N moPrP mimics a protein with H186 in a deprotonated state and with D201 in a protonated state. H186F-D201N moPrP shows a far-UV CD spectrum similar to that of wt moPrP under native conditions (Fig. S8). Although H186F-D201N moPrP was more stable than D201N moPrP (Fig. S9a), it was found to oligomerize as fast as D201N moPrP (Fig. S9b). Importantly, H186F-D201N moPrP was found to be completely misfolded in the pH range 2–5.2 (Fig. 4). This indicated that the protonation of just D201 alone was also sufficient for enabling the misfolding of moPrP. Not surprisingly, H186F-D201N moPrP showed structural changes, as measured by HDX-MS, similar to those shown by D201N moPrP (Fig. S10).

In the current study, it is shown that the protonation of either H186 or D201 has a critical effect on the stability, misfolding and oligomerization of moPrP. While the protonation of D201 leads to the disruption of the salt bridge R155-D201, protonation of H186 is likely to disrupt the electrostatic network between α1 and the α2-α3 regions [21,32,34,35]. Disruption of the salt bridge R155-D201 is likely to result in α1 moving away from the N-terminus of α3 and the loop between
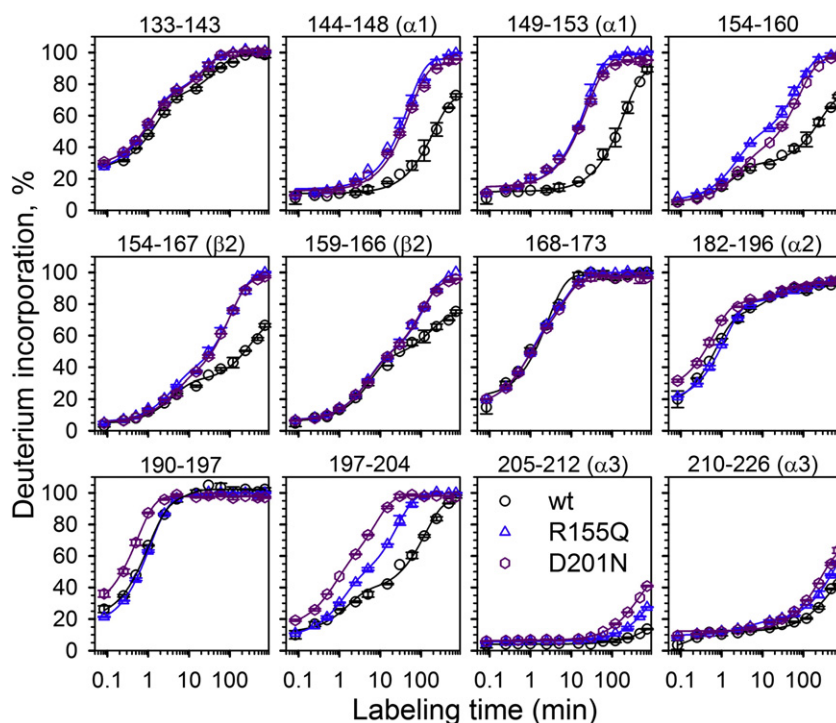
Fig. 7. Time course of HDX into different secondary structural regions of monomeric R155Q, D201N and wt moPrP at pH 4. Percent deuterium incorporation profiles at pH 4, 25 °C of selected sequence segments, are shown. Error bars represent the spread in data from two independent experiments. The lines through the data represent fits to either a monoexponential or a biexponential equation.
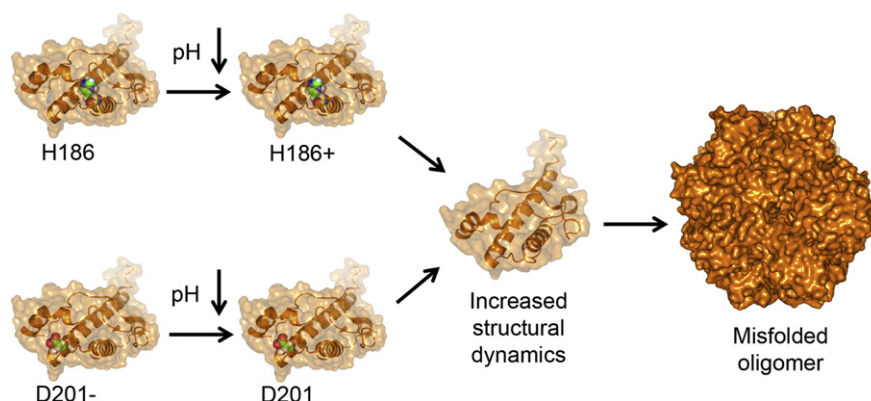
Fig. 8. Molecular model for the pH-induced misfolded oligomer formation by PrP. Protonation of H186 or D201 increase the structural dynamics of both α1 and the loop between α1 and β2. α1 is destabilized and appears to either unravel or move away from the structural core of the protein. These changes facilitate the pH-induced misfolding of PrP.

α2 and α3. Importantly, irrespective of the type of disruption caused by protonation of either H186 or D201, the structural consequences in the protein are very similar (Fig. 8). A previous study showed that D177N moPrP also undergoes similar structural changes [36]. Hence, these studies show that the protonation of D177, H186 or D201 leads to the same structural perturbations: destabilization of α1 and that of the loop between α1 and β2 because of either the movement of α1 away from the α2-α3 region or the unraveling of α1. Consequent to this structural perturbation, the intrinsic instability of α2 [39] would drive the misfolding of moPrP (Fig. 8) [11,36].

Several earlier studies support this mechanism of PrP misfolding. Computational studies carried out on either wt PrP or pathogenic mutant variants have suggested that α1 has high mobility and that its movement away from the α2-α3 region [26,40–42] eventually triggers the misfolding of the protein. A reduction in pH from 7.2 to 5.5 has been shown to lead to a reduction in the tertiary contacts between α1 and α3 in the pathogenic mutant variant V210I [43]. Structural studies on different misfolded forms of PrP show very similar results: α1 has unfolded, and α2 and α3 have converted into β-sheet [15,44,45]. Since these major conformational changes occur during the misfolding of PrP, the movement of α1 away from the α2-α3 region or the unraveling of α1 might be a necessary first step for its misfolding. Indeed, subdomain separation of β1-α1-β2 from α2-α3 has been shown to be a prerequisite for oligomerization: locking these two subdomains by disulfide linkage prevents oligomerization [46]. Recently, it has been shown that, in an acid-induced molten globule form of PrP at pH 2, the β1-α1-β2 region is preferentially unfolded, whereas the α2-α3 region remains marginally stable [47]. It is clear that destabilization/unraveling of α1 facilitates misfolding and oligomerization of mutant variants of moPrP and

that α1 has lost its structure in the misfolded oligomers formed at pH 4 [36]. Nevertheless, it is possible that, during the misfolding and oligomerization of wt moPrP at pH 4, α1 loses its structure only after the α2-α3 region undergoes conformational conversion. Kinetic studies are required to delineate the sequence of structural events that occur during the misfolding and oligomerization of PrP. These are currently under way.

Materials and Methods

Reagents

All reagents used for experiments were of the highest purity grade available from Sigma, unless otherwise specified. Urea and GdnHCl were purchased from USB and were of the highest purity grade.

Site-directed mutagenesis

The mutant variants of full-length moPrP were generated using the QuikChange® site-directed mutagenesis kit (Stratagene). Primers containing 1- to 2-nucleotide changes were obtained from Sigma. The mutations in the plasmids were confirmed by DNA sequencing.

Protein expression and purification

wt moPrP and all the mutant variants were expressed in *Escherichia coli* BL21 (DE3) codon plus (Stratagene) cells transformed with a pET17b plasmid containing the full-length sequence (23–231) of the moPrP gene. All the moPrP variants were purified as described previously [10,11]. No reducing agent was used during the whole protein purification procedure, and only one peak for the prion protein was observed during the reverse-phase chromatography step of protein purification. The protein

that eluted out in this peak was in the oxidized disulfide containing form as checked by MS (Waters Synapt G2 HD mass spectrometer). The purity of each moPrP variant preparation was confirmed by MS. Each moPrP variant showed an expected mass indicating that no chemical modification has taken place in any of the moPrP variants.

Far-UV CD measurements

Far-UV CD spectra were collected using a Jasco J-815 spectropolarimeter. Far-UV CD spectra were acquired using a protein concentration of 10 μM in a 1 mm cuvette, using a scan speed of 50 nm/min, a digital integration time of 2 s and a bandwidth of 1 nm. Far-UV CD spectra under native conditions were acquired in 10 mM sodium acetate buffer, pH 4, 25 °C. All the mutant proteins used in the current study showed far-UV CD spectra similar to that of wt moPrP under native conditions.

Urea-induced equilibrium unfolding studies

Urea-induced equilibrium unfolding transitions were carried out at pH 4 (in 10 mM sodium acetate buffer) and at pH 7 (in 50 mM Tris–HCl buffer) using 10 μM of protein. These studies were carried out in the same way as described earlier [11].

Thermal equilibrium unfolding studies

Thermal equilibrium unfolding transitions were monitored at pH 4 in 10 mM sodium acetate buffer using the change in the CD signal at 222 nm on the Jasco J-815 spectropolarimeter. 10 μM protein was used in a 1-mm cuvette, and the temperature scanning rate was 1 °C/min.

Misfolding at different pH values

The protein in 10 mM sodium acetate buffer (pH 4) was diluted twofold with 2× aggregation buffers (containing 300 mM NaCl) so that the protein was finally in 1× aggregation buffer containing 150 mM NaCl at the desired pH. 50 mM glycine-HCl buffer was used for pH values 2.1, 2.6, 3.1 and 3.6; 10 mM sodium acetate buffer was used for pH values 4.0, 4.4 and 4.6 while 50 mM Mes buffer was used for pH values 5.2 and 5.7. The samples were then incubated at 37 °C for 24 h. The final protein concentration used for all the experiments was 100 μM. D177N, H186F, H186R and D201N moPrP showed precipitation above pH 5.2 while H186F-D201N moPrP showed precipitation above pH 4.6. For studying the extent of misfolding, each sample was diluted to 10 μM in the same buffer in which it had been incubated for 24 h, and the far-UV CD spectrum was acquired within 10 min after dilution.

For analysis of the pH dependence of the CD signal, it was assumed that the formation of the misfolded oligomer (O) was coupled to the protonation, with dissociation constant K_a of a single critical residue in the monomeric protein (M).

$$M + H^+ \leftrightarrow MH^+ \leftrightarrow O$$

It is assumed that only MH$^+$ is competent to form O. In that case, the pH dependence is that of the protonation of M and is given by a transformation of the Henderson–Hasselbalch equation:

$$\text{Fraction MH}^+ = \frac{1}{1 + 10^{(\text{pH}-\text{p}K_a)}} \tag{1}$$

Fraction MH$^+$ is the fraction of protein protonated at the critical titrating residue. It is assumed that the MH$^+ \leftrightarrow$ O equilibrium completely favors O at the high protein concentration (100 μM) used. Then, Fraction MH$^+$ is equal to fraction misfolded oligomer.

Oligomerization and misfolding studies at pH 4 in the absence of chemical denaturants

The oligomerization and misfolding studies were carried out as described earlier [11]. Briefly, the protein in 10 mM sodium acetate buffer (pH 4) was diluted twofold with 2× aggregation buffer (10 mM sodium acetate buffer and 300 mM NaCl, pH 4) so that the protein was finally in 1× aggregation buffer (10 mM sodium acetate buffer and 150 mM NaCl, pH 4). The samples were then incubated at 37 °C. The final protein concentration used for all the experiments was 100 μM. Oligomerization at different timepoints was then monitored by SEC. For studying the extent of oligomerization, a 100-μL aliquot of the incubated sample was taken out and injected into a Waters Protein Pak 300-SW column using an Akta (GE) chromatography system kept at 25 °C. The column was equilibrated with 4 column volumes of 1× aggregation buffer at pH 4 (10 mM sodium acetate buffer and 150 mM NaCl), after several samples of oligomer had first been run through the column. In all subsequent SEC experiments, the amounts of oligomer and monomer that eluted out were found to account for all the protein that had been injected into the column. The areas under the monomer and oligomer peaks were calculated by fitting the SEC profiles (monitored by absorbance at 280 nm) to multiple Gaussian peaks, using Origin Pro 8. The fraction monomer left was calculated from the area under the monomer peak divided by the total area under all the peaks. The fraction oligomer formed was then calculated by subtracting fraction monomer from 1. Concurrently, the samples were diluted to 10 μM in 1× aggregation buffer and far-UV CD spectra were acquired.

For studying the misfolding rates of R155Q and D201N moPrP, misfolding experiments under the same conditions as described above were carried out using a water-jacketed 0.5-mm-quartz cuvette at 37 °C, and the kinetics were monitored by CD. Both the protein sample and 2× aggregation buffer were incubated at 37 °C before starting the reaction. The reaction was started by mixing 200 μM moPrP in equal amounts with 2× aggregation buffer and then immediately incubating it in the cuvette that was maintained at 37 °C, using a water bath. The time from the mixing of the protein with 2× aggregation buffer to the first reading was ~40 s. Since the change in CD signal at 228 nm, as native monomer converts into misfolded oligomers, is substantial, the time course of the change in the CD signal was studied at 228 nm, where the signal to noise ratio is better than at lower wavelengths.

Oligomerization and misfolding at pH 4 in the presence of chemical denaturants

These studies were carried out as described earlier [11]. The final oligomerization condition was 10 mM sodium acetate buffer, 150 mM NaCl, 1 M GdnHCl, 3 M urea (pH 4, at 37 °C) and 100 μM protein concentration.

HDX-MS measurements

The peptide map of the moPrP variants was generated as described earlier [15]. 10 mM sodium acetate buffer prepared in D_2O was used as a labeling buffer for pH 4 (corrected for isotope effect) studies while 10 mM Tris–DCl buffer prepared in D_2O was used as a labeling buffer for pH 7 (corrected for isotope effect) studies. HDX-MS measurements were carried out as described earlier [11]. Briefly, to initiate deuterium labeling, a 100 μM protein sample was diluted 20-fold into the labeling buffer so that the protein was in 95% D_2O and incubated it at 25 °C. At different times of labeling, 50 μL of aliquot was withdrawn from the labeling reaction and was mixed with 50 μL of ice-cold 20 mM glycine-HCl buffer at pH 2.5 to quench the labeling. The sample was then immediately injected into the HDX module (Waters) coupled with the nano Acquity UPLC for online pepsin digestion using an immobilized pepsin cartridge (Applied Biosystems). Further processing of the sample for mass determination using a Waters Synapt G2 mass spectrometer was carried out as described earlier [11,15].

Acknowledgments

Appendix A. Supplementary data

Supplementary data to this article can be found online at http://dx.doi.org/10.1016/j.jmb.2016.01.030.

References

[1] S.B. Prusiner, Prion diseases and the BSE crisis, Science 278 (1997) 245–251.

[2] R. Diaz-Espinoza, C. Soto, High-resolution structure of infectious prion protein: The final frontier, Nat. Struct. Mol. Biol. 19 (2012) 370–377.

[3] Z.E. Anaya, et al., Recovery of small infectious PrPres aggregates from prion-infected cultured cells, J. Biol. Chem. 286 (2011) 8141–8148.

[4] P. Tixador, et al., The physical relationship between infectivity and prion protein aggregates is strain-dependent, PLoS Pathog. 6 (2010), e1000859.

[5] M. Kristiansen, et al., Disease-associated prion protein oligomers inhibit the 26S proteasome, Mol. Cell 26 (2007) 175–188.

[6] S. Simoneau, et al., *In vitro* and *in vivo* neurotoxicity of prion protein oligomers, PLoS Pathog. 3 (2007), e125.

[7] Y.P. Choi, A. Gröner, J.W. Ironside, M.W. Head, Correlation of polydispersed prion protein and characteristic pathology in the thalamus in variant Creutzfeldt–Jakob Disease: Implication of small oligomeric species, Brain Pathol. 21 (2011) 298–307.

[8] C. Kim, et al., Small protease sensitive oligomers of PrPSc in distinct human prions determine conversion rate of PrPC, PLoS Pathog. 8 (2012), e1002835.

[9] G. Sajnani, et al., PK-sensitive PrPSc is infectious and shares basic structural features with PK-resistant PrPSc, PLoS Pathog. 8 (2012), e1002547.

[10] S. Jain, J.B. Udgaonkar, Evidence for stepwise formation of amyloid fibrils by the mouse prion protein, J. Mol. Biol. 382 (2008) 1228–1241.

[11] J. Singh, H. Kumar, A.T. Sabareesan, J.B. Udgaonkar, Rational stabilization of helix 2 of the prion protein prevents its misfolding and oligomerization, J. Am. Chem. Soc. 136 (2014) 16704–16707.

[12] N. Sanghera, M. Wall, C. Vénien-Bryan, T.J. Pinheiro, Globular and pre-fibrillar prion aggregates are toxic to neuronal cells and perturb their electrophysiology, Biochim. Biophys. Acta 1784 (2008) 873–881.

[13] M.Q. Khan, et al., Prion disease susceptibility is affected by β-structure folding propensity and local side-chain interactions in PrP, Proc. Natl. Acad. Sci. U. S. A. 107 (2010) 19808–19813.

[14] J.F. Chich, et al., Vesicle permeabilization by purified soluble oligomers of prion protein: A comparative study of the

interaction of oligomers and monomers with lipid membranes, J. Mol. Biol. 397 (2010) 1017–1030.

[15] J. Singh, A.T. Sabareesan, M.K. Mathew, J.B. Udgaonkar, Development of the structural core and of conformational heterogeneity during the conversion of oligomers of the mouse prion protein to worm like amyloid fibrils, J. Mol. Biol. 423 (2012) 217–231.

[16] J. Singh, J.B. Udgaonkar, Molecular mechanism of the misfolding and oligomerization of the prion protein: Current understanding and its implications, Biochemistry 54 (2015) 4431–4442.

[17] I.V. Baskakov, G. Legname, M.A. Baldwin, S.B. Prusiner, F.E. Cohen, Pathway complexity of prion protein assembly into amyloid, J. Biol. Chem. 277 (2002) 21140–21148.

[18] B. Chesebro, et al., Anchorless prion protein results in infectious amyloid disease without clinical scrapie, Science 308 (2005) 1435–1439.

[19] D.R. Borchelt, A. Taraboulos, S.B. Prusiner, Evidence for synthesis of scrapie prion proteins in the endocytic pathway, J. Biol. Chem. 267 (1992) 16188–16199.

[20] J.E. Arnold, et al., The abnormal isoform of the prion protein accumulates in late-endosome-like organelles in scrapie-infected mouse-brain, J. Pathol. 176 (1995) 403–411.

[21] E. Langella, R. Improta, O. Crescenzi, V. Barone, Assessing the acid–base and conformational properties of histidine residues in human prion protein (125–228) by means of pK_a calculations and molecular dynamics simulations, Proteins 64 (2006) 167–177.

[22] S.H. Bae, et al., Prion proteins with pathogenic and protective mutations show similar structure and dynamics, Biochemistry 48 (2009) 8120–8128.

[23] L. Cervenakova, et al., Novel PRNP sequence variant associated with familial encephalopathy, Am. J. Med. Genet. 88 (1999) 653–656.

[24] L.L. Hosszu, et al., The H187R mutation of the human prion protein induces conversion of recombinant prion protein to the PrPSc-like form, Biochemistry 49 (2010) 8729–8738.

[25] M.W. van der Kamp, V. Daggett, The consequences of pathogenic mutations to the human prion protein, Protein Eng. Des. Sel. 22 (2009) 461–468.

[26] M.L. DeMarco, V. Daggett, Molecular mechanism for low pH triggered misfolding of the human prion protein, Biochemistry 46 (2007) 3045–3054.

[27] W.C. Guest, N.R. Cashman, S.S. Plotkin, Electrostatics in the stability and misfolding of the prion protein: Salt bridges, self energy, and solvation, Biochem. Cell Biol. 88 (2010) 371–381.

[28] S. Hadži, A. Ondračka, R. Jerala, I. Hafner-Bratkovič, Pathological mutations H187R and E196K facilitate subdomain separation and prion protein conversion by destabilization of the native structure, FASEB J. 29 (2015) 882–893.

[29] J. Singh, J.B. Udgaonkar, The pathogenic mutation T182A converts the prion protein into a molten globule-like conformation whose misfolding to oligomers but not to fibrils is drastically accelerated, Biochemistry 55 (2016) 459–469.

[30] F. Sokolowski, et al., Formation of critical oligomers is a key event during conformational transition of recombinant Syrian hamster prion protein, J. Biol. Chem. 278 (2003) 40481–40492.

[31] H. Rezaei, et al., Sequential generation of two structurally distinct ovine prion protein soluble oligomers displaying different biochemical reactivities, J. Mol. Biol. 347 (2005) 665–679.

[32] E. Langella, R. Improta, V. Barone, Checking the pH-induced conformational transition of prion protein by molecular dynamics simulations: Effect of protonation of histidine residues, Biophys. J. 87 (2004) 3623–3632.

[33] M.W. van der Kamp, V. Daggett, Influence of pH on the human prion protein: Insights into the early steps of misfolding, Biophys. J. 99 (2010) 2289–2298.

[34] S.R. Campos, M. Machuqueiro, A.M. Baptista, Constant-pH molecular dynamics simulations reveal a β-rich form of the human prion protein, J. Phys. Chem. B 114 (2010) 12692–12700.

[35] J. Garrec, I. Tavernelli, U. Rothlisberger, Two misfolding routes for the prion protein around pH 4.5, PLoS Comput. Biol. 9 (2013) e1003057.

[36] J. Singh, J.B. Udgaonkar, Structural effects of multiple pathogenic mutations suggest a model for the initiation of misfolding of the prion protein, Angew. Chem. Int. Ed. 54 (2015) 7529–7533.

[37] A.C. Apetri, D.L. Vanik, W.K. Surewicz, Polymorphism at residue 129 modulates the conformational conversion of the D178N variant of human prion protein 90–231, Biochemistry 44 (2005) 15880–15888.

[38] S. Liemann, R. Glockshuber, Influence of amino acid substitutions related to inherited human prion diseases on the thermodynamic stability of the cellular prion protein, Biochemistry 38 (1999) 3258–3267.

[39] R.I. Dima, D. Thirumalai, Exploring the propensities of helices in PrPC to form β sheet using NMR Structures and sequence alignments, Biophys. J. 83 (2002) 1268–1280.

[40] A. De Simone, A. Zagari, P. Derreumaux, Structural and hydration properties of the partially unfolded states of the prion protein, Biophys. J. 93 (2007) 1284–1292.

[41] L. Zhong, Exposure of hydrophobic core in human prion protein pathogenic mutant H187R, J. Biomol. Struct. Dyn. 28 (2010) 355–361.

[42] E. Behmard, P. Abdolmaleki, E.B. Asadabadi, S. Jahandideh, Prevalent mutations of human prion protein: A molecular modeling and molecular dynamics study, J. Biomol. Struct. Dyn. 29 (2011) 379–389.

[43] I. Biljan, G. Ilc, G. Giachin, J. Plavec, G. Legname, Structural rearrangements at physiological pH: Nuclear magnetic resonance insights from the V210I human prion protein mutant, Biochemistry 51 (2012) 7465–7474.

[44] X. Lu, P.L. Wintrode, W.K. Surewicz, β-sheet core of human prion protein amyloid fibrils as determined by hydrogen/deuterium exchange, Proc. Natl. Acad. Sci. U. S. A. 104 (2007) 1510–1515.

[45] J. Singh, J.B. Udgaonkar, Dissection of conformational conversion events during prion amyloid fibril formation using hydrogen exchange and mass spectrometry, J. Mol. Biol. 425 (2013) 3510–3521.

[46] F. Eghiaian, et al., Diversity in prion protein oligomerization pathways results from domain expansion as revealed by hydrogen/deuterium exchange and disulfide linkage, Proc. Natl. Acad. Sci. U. S. A. 104 (2007) 7414–7419.

[47] R.P. Honda, K.I. Yamaguchi, K. Kuwata, Acid-induced molten globule state of a prion protein: Crucial role of strand 1-helix 1-strand 2 segment, J. Biol. Chem. 289 (2014) 30355–30363.